

THE SWEDISH RESEARCH COUNCILS' LABORATORY

Studsvik, Fack  
S-611 01 Nyköping 1  
Sweden

Research report  
LF-77  
1976

---

ENERGY SPECTRA OF DELAYED NEUTRONS FROM THE PRECURSORS

$^{79}\text{(Zn,Ga)}$ ,  $^{80}\text{Ga}$ ,  $^{81}\text{Ga}$ ,  $^{94}\text{Rb}$ ,  $^{95}\text{Rb}$ ,  $^{129}\text{In}$ , and  $^{130}\text{In}$

G Rudstam and E Lund

The Swedish Research Councils' Laboratory,  
Studsvik, Fack, S-611 01 Nyköping, Sweden

# ENERGY SPECTRA OF DELAYED NEUTRONS FROM THE PRECURSORS

$^{79}\text{(Zn,Ga)}$ ,  $^{80}\text{Ga}$ ,  $^{81}\text{Ga}$ ,  $^{94}\text{Rb}$ ,  $^{95}\text{Rb}$ ,  $^{129}\text{In}$ , and  $^{130}\text{In}$

by

G Rudstam and E Lund

The Swedish Research Councils' Laboratory, Studsvik,  
Nyköping, Sweden

Abstract: Energy spectra of delayed neutrons from the mass-separated fission products  $^{79}\text{(Zn,Ga)}$ ,  $^{80,81}\text{Ga}$ ,  $^{94,95}\text{Rb}$  and  $^{129,130}\text{In}$  have been measured. The neutron envelopes are deduced and compared to predicted envelopes using various mass formulae. The agreement is good for all precursors except for  $^{79}\text{(Zn,Ga)}$  whose predicted neutron window is too narrow to reproduce the experimental results.

## 1. INTRODUCTION

The energy distribution of delayed neutrons from mass separated fission products has been reported in three articles covering together 17 cases<sup>1-3)</sup>. This article concludes the series of measurements on fission products obtained at the OSIRIS isotope-separator-on-line facility<sup>4)</sup> with its present ion-source arrangement. The precursors studied are  $^{79}\text{(Zn,Ga)}$ ,  $^{80,81}\text{Ga}$ ,  $^{94,95}\text{Rb}$ , and  $^{129,130}\text{In}$ , thus essentially odd-Z elements. In the case of rubidium the final nuclei have an excess of neutrons, 5 and 6, respectively, above the 50-shell. These cases naturally belong to the series treated in refs.<sup>2)</sup> and <sup>3)</sup>. In contrast to this, the final nuclei in the gallium and indium cases contain 2-4 neutrons below the 50- and 82-shells, respectively, i.e. the emitters belong to a type not encountered before in the series of measurements at this laboratory.

The techniques used in the measurements are described in detail in an earlier report<sup>5)</sup>. A neutron spectrometer consisting of a cylindrical gridded ionization chamber was used at the on-line position of the isotope separator, and the samples were collected on an aluminized mylar tape moving with a speed of about 5 mm/s to remove decay products, and viewed through a bismuth absorber of thickness 10 mm to decrease the gamma pile-up in the spectrometer.

The precursor  $^{81}\text{Ga}$  gives a neutron spectrum with pronounced fine structure. Such a structure is much less dominant in the other cases. The gross structure has been analyzed according to the method developed in ref.<sup>6)</sup>. According to this method the neutron envelope can be written

$$P(E_n)dE_n = \sum_l C_l S_l(E_n) \frac{e^{2\sqrt{a(E-P)}}}{(E-P)^{5/4}} (Q_\beta - E)^5 dE_n, \quad (1)$$

where  $E_n$  is the neutron energy,  $E$  the excitation energy of the beta decay product,  $S_l(E_n)$  the neutron branching ratio of neutrons of wave number  $l$ , i.e. the ratio  $T_l/(T_l+K_l)$  where  $T_l$  is the neutron transmission constant and  $K_l$  is a constant proportional to the gamma width. This constant is adjusted to force the neutron energy distribution to peak at 10 keV, 200 keV, 400 keV, and 600 keV for  $l = 1, 2, 3$ , and 4, respectively, for light fission products, and at 10 keV, 10 keV, 300 keV, 600 keV, and 1000 keV for  $l = 0, 1, 2, 3$ , and 4 respectively, for heavy fission products (cf. ref.<sup>6)</sup>). The parameters  $a$  and  $P$  (pairing energy) are those entering in the usual form of the level density formula (cf., for instance, ref.<sup>2)</sup>). Finally,  $C_l$  are normalization constants.

The sum is taken over the wave numbers of importance for the neutron emission.

The parameters  $a$  and  $P$  are obtained from ref.<sup>7)</sup>, and the  $Q_\beta$  values from ref.<sup>10)</sup>. The neutron binding energy is then adjusted to obtain agreement between experimental and calculated envelopes.

The procedure outlined above is sensitive to the "neutron window", i.e. the difference between the total decay energy of the precursor and the neutron binding energy of the daughter. The agreement between neutron windows deduced in the present work and neutron windows from published mass data<sup>11-15)</sup> is satisfactory in all cases except for  $^{79}(\text{Zn}, \text{Ga})$ , where the window obtained in the present work is much larger than the mass formula predictions.

## 2. EXPERIMENTAL RESULTS

### 2.1 The precursor $^{79}(\text{Zn}, \text{Ga})$

Delayed-neutron multiscaling of samples of mass 79 indicates only one component of half-life  $2.63 \pm 0.09 \text{ s}$ <sup>16)</sup> in fair agreement with the value  $3.00 \pm 0.09 \text{ s}$  obtained by beta counting<sup>17)</sup>. It is not

ascertained which isobar this activity belongs to, however. According to various mass formulae both  $^{79}\text{Zn}$  and  $^{79}\text{Ga}$  are expected to be neutron precursors. For the time being, this question must be left open, and the activity is consequently denoted  $^{79}(\text{Zn,Ga})$  (cf. also the discussion in ref. <sup>16)</sup>).

The pulse spectrum obtained is shown in Fig. 1(a) together with the neutron spectrum resulting from a conversion of the pulse spectrum applying the response function of the spectrometer in an iterative manner <sup>18)</sup>. The neutron energy spectrum is shown in Fig. 1 (b) as a histogram with each step corresponding 10 keV.

The statistics of the measurement is apparently not good enough to reveal any fine structure.

Assuming the ground state spin of  $^{79}\text{Ga}$  to be  $3/2^-$  <sup>19)</sup> both p-wave and f-wave neutron emission to the ground state of the final nucleus  $^{78}\text{Ge}$  are possible after allowed beta decay of the precursor. Thus, the neutron spectrum may be expected to contain these two branches. Using the experimental  $Q_\beta$ -value of  $6.76 \pm 0.08$  MeV <sup>8)</sup> and the parameters from Table 1 and adjusting the  $B_n$ -value to 5.15 MeV the experimental neutron distribution can be well reproduced by adding one p-wave component and one f-wave component in the ratio 2:1 (this ratio is not obtained very accurately in the analysis) as is seen by the dotted curve in Fig. 1(b).

Table 2 contains predicted neutron windows. These indicate a considerably lower neutron window than obtained here, or  $0.36$  MeV <sup>11)</sup>, a negative value (no delayed neutrons) <sup>12)</sup>,  $0.79$  MeV <sup>13)</sup>, and  $0.39$  MeV <sup>14)</sup> compared to  $1.61$  MeV. It should be noted, however, that the  $B_n$ -value deduced is compatible with the value  $5.68 \pm 0.64$  MeV given by Wapstra and Gove <sup>15)</sup>.

The disagreement between the present experiment and mass formula predictions concerning the width of the neutron window is not removed if the delayed neutrons are ascribed to  $^{79}\text{Zn}$  rather than to  $^{79}\text{Ga}$ . In fact, two of the mass formulae chosen for the comparison, or refs. <sup>12)</sup> and <sup>14)</sup>, predict a negative window. The others give  $0.61$  MeV <sup>11)</sup> and  $1.03$  MeV <sup>13)</sup>.

## 2.2 The precursor $^{80}\text{Ga}$

The activity can be ascribed to  $^{80}\text{Ga}$  (cf. ref. <sup>16)</sup>). The statistics was not very good, and no fine structure is revealed in the pulse spectrum shown in Fig. 2(a). The corresponding neutron spectrum is shown in Fig. 2(b) as a histogram with each step corresponding to 10 keV.

The experimental  $Q_{\beta}$ -value is  $\geq 8.6 \pm 0.6$  MeV with the equality sign valid if the gate energy 2853 MeV used in the determination corresponds to a level in  $^{80}\text{Ge}$  <sup>8)</sup>. With  $Q_{\beta}$  put equal to 8.60 MeV and with other parameters taken from Table 1, Eq. (1) gives an envelope which agrees well with the experimental spectrum for a neutron binding energy adjusted to 7.40 MeV as is seen from Fig. 2(b). In this case the spectrum is composed to three branches. With the assumption of the spin values  $1^+$  for  $^{80}\text{Ga}$  and  $7/2^+$  for  $^{79}\text{Ge}$  (cf. ref. <sup>19)</sup>) one finds that only d-wave and g-wave ground state neutron emission are possible after allowed beta-decay of the precursor. This does not explain the presence of low-energy neutrons, however, and therefore an s-wave branch leading to a hypothetical excited level at about 600 keV has been arbitrarily added. It may be noted that preliminary work at this laboratory has indicated excited levels at 512 and 607 keV in the scheme of  $^{79}\text{Ge}$  <sup>20)</sup>.

The resulting neutron window is 1.20 MeV which is in the range of the mass formula predictions 0.94 MeV <sup>11)</sup>, 0.27 MeV <sup>12)</sup>, 1.69 MeV <sup>13)</sup>, and 1.12 MeV <sup>14)</sup>.

The  $B_{\beta}$ -value 7.40 MeV is lower than the predictions from the mass formulae <sup>11-14)</sup>. In view of the uncertainty of the  $Q_{\beta}$ -value this disagreement cannot be considered as serious, however.

## 2.3 The precursor $^{81}\text{Ga}$

Only one delayed-neutron precursor, presumably  $^{81}\text{Ga}$ , has been found at this mass <sup>16)</sup>. The statistics of the measurement was better than in the preceding cases, and some peaks, notably at 80, 140, 240, 290, 330, 380, 500, and 540 keV are seen in the neutron spectrum shown in Fig. 3.

In analogy with the precursor  $^{79}\text{Ga}$  one might expect p-wave and f-wave ground-state neutron emission, but a p-wave component suffices to describe the remainder obtained after subtracting the peaks as is seen from Fig. 3(b). The parameters used are given in Table 1. In this case the  $Q$ -value has been determined to  $\geq 7.23 \pm 0.19$  MeV with the equality sign valid under the assumption that the energy 2443 MeV corresponds to a level in  $^{81}\text{Ge}$ <sup>8)</sup>. The  $Q$ -value 7.23 MeV gives an envelope which reproduces the experimental spectrum for a  $B_n$ -value of 5.15 MeV. The neutron window of 2.08 MeV, thus obtained, is somewhat larger than the predictions 1.22 MeV<sup>11)</sup>, 0.74 MeV<sup>12)</sup>, 1.65 MeV<sup>13)</sup>, and 1.18 MeV<sup>14)</sup>.

The  $B_n$ -value 5.15 MeV agrees reasonably well with the average value deduced from the mass formulae of refs. <sup>11-14)</sup>, which is 5.40 MeV.

#### 2.4 The precursor $^{94}\text{Rb}$

The delayed-neutron emission at mass 94 is completely dominated by  $^{94}\text{Rb}$ <sup>16)</sup>. Except for an indication of a peak at 130 keV and a clear evidence for a wide peak at 300 keV, no fine structure is statistically ascertained in the neutron spectrum. The pulse distribution and the delayed-neutron spectrum are shown in Fig. 4.

The spin of  $^{94}\text{Rb}$  is assumed to be  $4^-$ <sup>19)</sup> and that of  $^{93}\text{Sr}$   $5/2^+$  (in analogy with  $^{89,91}\text{Sr}$ ). Then both p-wave and f-wave neutron emission to the ground state are possible after allowed beta decay of the precursor. It is not possible to fit the experimental neutron energy distribution using only these components, however. If the high energy end is fitted there is a serious mismatch at the low-energy end, and vice versa. A considerable improvement is obtained assuming a substantial population of excited states of the final nucleus. This is shown in Fig. 4(b) where only two components have been retained - an f-wave component to the ground state of the final nucleus and a p-wave component feeding a hypothetical excited state at about 1 MeV.

The calculation was done using the experimental  $Q_{\beta}$ -value of  $10.14 \pm 0.25$  MeV<sup>9)</sup>, the parameters of Table 1, and a  $B_n$ -value adjusted to 7.90 MeV. The corresponding neutron window of 2.24 MeV should be compared to 2.28 MeV<sup>11)</sup>, 1.06 MeV<sup>12)</sup>, 2.94 MeV<sup>13)</sup>, and 2.85 MeV<sup>14)</sup>. Apparently, it falls within the range of these predictions.

The  $B_n$ -value 7.90 MeV is about 1 MeV higher than the value  $6.86 \pm 0.23$  MeV given by Wapstra and Gove<sup>15)</sup>. It should be noted, however, that the binding energy was deduced assuming the experimental  $Q_{\beta}$ -value to be correct. All that can be safely stated is that the shape of the delayed-neutron spectrum is incompatible with the neutron window  $3.28 \pm 0.35$  MeV arising from the mass data of refs. 9) and 15) (unless ground state neutron branches are lacking).

#### 2.5 The precursor $^{95}\text{Rb}$

The pulse distribution and the resulting neutron spectrum are shown in Fig. 5. The statistics is rather poor, and it is not possible to reveal any fine structure peaks.

Both p-wave and f-wave neutron emission to the ground state of  $^{94}\text{Sr}$  following allowed beta decay of the precursor are possible. As in the preceding case a good fit to the experimental spectrum requires feeding of excited states in the final nucleus. As is seen in Fig. 5(b) an excellent fit is obtained assuming an f-wave component to the ground state and a p-wave component to a hypothetical excited state at about 600 keV. The experimental  $Q_{\beta}$ -value of  $8.59 \pm 0.30$  MeV<sup>9)</sup> is used, the  $B_n$ -value is adjusted to 5.90 MeV, and other parameters are given in Table 1. The resulting neutron window is 2.69 MeV to be compared to the mass formula predictions  $3.23$  MeV<sup>11)</sup>,  $1.89$  MeV<sup>12)</sup>,  $3.85$  MeV<sup>13)</sup>, and  $3.33$  MeV<sup>14)</sup>. The predicted values vary greatly, with one value lower and the others higher than the present result.

#### 2.6 The precursor $^{129}\text{In}$

There are two isomers of indium which apparently contribute to the neutron spectrum. Their half-lives are  $0.99 \pm 0.02$  s and  $2.5 \pm 0.2$  s, respectively, as found by delayed-neutron counting<sup>21)</sup>. Although the moving tape will enhance the more short-lived component somewhat, the spectrum measured is obviously composite.

The pulse spectrum and the neutron spectrum are shown in Fig. 6. Indications of peaks are seen at energies 690 and 860 keV.

The presence of two isomers of spins presumably,  $1/2^-$  and  $9/2^+$  <sup>19)</sup> makes possible p-wave, f-wave and g-wave ground state neutron emission after allowed beta decay of the precursors. Furthermore, the lowest excited state of  $^{128}\text{Sn}$  is known to be a  $2^+$ -level at 1169 keV <sup>22)</sup>, and this level could be fed by p-wave, d-wave, and f-wave neutrons after allowed beta decay. Thus, the situation is quite complicated with many neutron branches to be expected.

A combination of two branches, p-wave and d-wave neutrons feeding the excited state at 1169 keV and another two branches, f-wave and g-wave neutrons, feeding the ground state of  $^{128}\text{Sn}$  gives an excellent fit to the experimental spectrum as is seen in Fig. 6(b). The experimental  $Q$ -value of  $7.52 \pm 0.12$  MeV <sup>8)</sup> (corresponding to the 0.99 s activity) and the parameters of Table 1 have been used, and the  $B_n$ -value was adjusted to 5.60 MeV. The resulting neutron window is 1.92 MeV in excellent agreement with the mass formula predictions 1.99 MeV <sup>11)</sup>, 1.47 MeV <sup>12)</sup>, 1.70 MeV <sup>13)</sup>, and 1.97 MeV <sup>14)</sup>.

## 2.7 The precursor $^{130}\text{In}$

According to delayed-neutron counting only one contributing activity should be present, with a half-life of  $0.58 \pm 0.01$  s <sup>21)</sup>. The spectra obtained are shown in Fig. 7. The statistics are too poor to reveal any fine structure, except for a weak indication around 700 keV.

The spin of  $^{130}\text{In}$  is assumed to be  $5^+$  <sup>10)</sup>. In the final nucleus  $^{129}\text{Sn}$  the ground state spin is  $3/2^+$  <sup>23)</sup>. Several excited levels are known, among them one at 1044 keV assigned to spin  $7/2^+$ . Apparently, the ground state can be fed by d-wave and g-wave neutron emission, and the above-mentioned excited level by s-wave emission as well, following allowed beta decay. There are also negative parity states, the most important one being an isomeric state at 35 keV with spin  $11/2^-$ . Another level at 764 keV is tentatively assigned spin  $9/2^-$  <sup>23)</sup>. Both these levels can be populated via p-wave and f-wave neutron emission after allowed beta decay. Thus, a situation arises which is similar to the one of the preceding case: a large variety of neutron branches are possible. Four of these branches have been chosen to describe the spectrum, or s-wave and d-wave neutrons feeding the excited state at 1044 keV, and f-wave and g-wave neutrons feeding the



ground state of  $^{129}_{111}\text{Sn}$ . The fit, obtained with the experimental  $Q_{\beta}$ -value of  $9.3 \pm 0.5$  MeV, is shown in Fig.7(b). The neutron window is 1.90 MeV, in excellent agreement with the mass formula predictions  $2.27$  MeV<sup>11)</sup>,  $1.87$  MeV<sup>12)</sup>,  $2.03$  MeV<sup>13)</sup>, and  $2.30$  MeV<sup>14)</sup>.

### 3. DISCUSSION

All the neutron emitters investigated earlier in the series of measurements at this laboratory have one or more neutrons in excess of the 50- or 82 neutron shells. With the exception of  $^{94,95}\text{Rb}$  the emitters studied in the present work have a deficit of 2 - 4 neutrons. This means in general larger neutron separation energies and thus neutron emission from higher excitation energy bands in the beta decay daughter. Then, fine structure in the neutron spectra is not to be expected because of the higher level densities connected to larger excitation energies. Still, the neutron spectrum of the precursor  $^{81}\text{Ga}$  exhibits a pronounced fine structure comprising several peaks, and indications of some structure are also found in the spectra of the indium isotopes. The poor statistics prevent any conclusions on fine structure in the other cases.

The neutron spectra have been analyzed by a method originally designed to obtaining useful descriptions of the spectra to be introduced in calculations of the resulting neutron spectra in nuclear fuel.<sup>6)</sup> The relative contributions from different neutron wave numbers have been varied in order to reproduce the experimental spectra as well as possible. Also, decay modes to hypothetical or known excited states in the final nuclei have sometimes been postulated to improve the fit. This means a certain amount of arbitrariness especially where several branches have been used, and the results have therefore not been used for calculating quantities such as the neutron branching ratios as was done in refs.<sup>1-3)</sup>. The fitting procedure is quite sensitive to one specific quantity, however, or the neutron window which can probably be determined within 0.1 - 0.2 MeV. This quantity therefore lends itself well to comparisons with predictions from different mass formulae. Such comparisons are done in Table 2. In general, the mass formula data describe the neutron spectra quite well. An exception is  $^{79}(\text{Zn},\text{Ga})$  where the neutron spectrum extends to a considerably higher energy than expected. To a lesser degree, this also holds for  $^{81}\text{Ga}$ .

ACKNOWLEDGEMENTS

The assistance of Mr L Jacobsson and Mr O C Jonsson is gratefully acknowledged.

The work has been supported by the Swedish Council for Atomic Research.

## REFERENCES

- 1) S Shalev and G Rudstam, Nucl. Phys. A230 (1974) 153.
- 2) G Rudstam and S Shalev, Nucl. Phys. A235 (1974) 397.
- 3) S Shalev and G Rudstam, to be published in Nucl. Phys.
- 4) S Borg, I Bergstrom, G B Holm, B Rydberg, L E De Geer, G Rudstam, B Grapengiesser, E Lund, and L Westgaard, Nucl. Instr. Methods 91 (1971) 109.
- 5) G Rudstam, S Shalev, and O C Jonsson, Nucl. Instr. Methods 120 (1974) 333.
- 6) G Rudstam, The Swedish Research Councils' Laboratory, Report LF-70 (1976).
- 7) J W Truran, A G W Cameron and G Hilf, CERN Report 70-30 (1970) p.275.
- 8) K Aleklett, E Lund, G Nyman, and G Rudstam, The Swedish Research Councils' Laboratory Report LF-71 (1976). Proceedings of the 3rd International Conference on Nuclei far from Stability, Cargèse, Corsica 19 - 26 May 1976.
- 9) M I Macias-Marques, R Foucher, M Cailliau, and J Belhassen, CERN Report 70-30 (1970) p.321.
- 10) A Kerek, G B Holm, S Borg, and P Carlé, Nucl. Phys. A209 (1973)520.
- 11) G T Garvey, W J Grace, R L Jaffe, I Talmi, and I Kelson, Revs. Mod. Phys. 41 (1969) S1.
- 12) W D Myers and W J Swiatecki, Droplet Model Mass Table (1975), (unpublished).
- 13) S Liran and N Zeldes, Institut für Kernphysik, Technische Hochschule Darmstadt Report IKDA 75/14 (1975) (unpublished).
- 14) P A Seeger and W M Howard, Nucl. Phys. A238 (1975) 491 and American Report LA-5750.
- 15) A H Wapstra and N B Gove, Nucl. Data Tables 9 (1971) 267.
- 16) E Lund and G Rudstam, Phys. Rev. C13 (1976) 321.
- 17) B Grapengiesser, E Lund, and G Rudstam, J. Inorg. Nucl. Ch 36 (1974)2409.
- 18) G Rudstam, Thw Swedish Research Councils' Laboratory Report LF-57 (1974).
- 19) K Aleklett, G Nyman, and G Rudstam, Nucl. Phys. A246 (1975)425.
- 20) T Matsushigue and L Matsushigue, unpublished work (1972).
- 21) E Lund and G Rudstam, Phys. Rev. C13 (1976) 1544.
- 22) B Fogelberg, private communication (1976)
- 23) L E De Geer and G B Holm, The Research Institute for Physics, Stockholm, Annual Report 1974, p. 102.
- 24) M Asghar, J P Gautheron, G Bailleul, J P Bocquet, J Greif, H Schrader, G Siegert, C Ristori, J Grançon, and G I Crawford, Nucl. Phys. A247 (1975) 359.

TABLE 1  
Parameters describing the energy spectrum of the delayed neutrons

Precursor	$\lambda^a)$ MeV <sup>-1</sup>	$\rho^a)$ MeV	$Q_n^b)$ MeV	$B_n$ MeV (adjusted)	$l$	Energy of level fed in neutron decay	Relative intensity	$K_l$
<sup>79</sup> Ga	10.03	1.201	6.76 <sup>b)</sup>	5.15	1	0	67	0.00010
					3	0	33	0.00066
<sup>80</sup> Ga	9.70	2.542	8.60 <sup>b)</sup>	7.40	0	0.6	50	0.0277
					2	0	30	0.0032
					4	0	20	0.0001
<sup>81</sup> Ga	9.25	1.201	7.23 <sup>b)</sup>	5.15	1	0	68 <sup>e)</sup>	0.0001
<sup>94</sup> Rb	12.49	2.367	10.14 <sup>c)</sup>	7.90	1	1.0	77	0.00010
					3	0	23	0.00026
<sup>95</sup> Rb	13.04	1.272	8.59 <sup>c)</sup>	5.90	1	0.6	60	0.00010
					3	0	40	0.00013
<sup>129</sup> In	10.93	1.307	7.52 <sup>b)</sup>	5.60	1	1.169	30	0.00012
					2	1.169	30	1.0
					3	0	25	0.0240
					4	0	15	0.149
<sup>130</sup> In	10.39	2.369	9.30 <sup>d)</sup>	7.40	0	1.044	35	0.0169
					2	1.044	30	1.0
					3	0.035	20	0.0275
					4	0	15	0.0100

a) Ref. 7)

b) Ref. 8)

c) Ref. 9)

d) Ref. 10)

e) In addition to the gross structure component there are fine structure peaks of energies (in MeV) 0.08 (3.8%), 0.14 (5.5%), 0.24 (3.4%), 0.29 (3.6%), 0.33 (8.0%), 0.38 (4.0%), 0.44 (1.8%), 0.50 (1.0%), and 0.54 (1.2%).

TABLE 2

Comparison between neutron windows determined in the present work and predictions from mass formulae

Precursor	$(Q - B_n)$ , MeV				
	This work	Garvey et al. <sup>a)</sup>	Myers and Swiatecki <sup>b)</sup>	Liran and Zeldes <sup>c)</sup>	Seeger and Howard <sup>d)</sup>
<sup>79</sup> Ga	1.61	0.36	-0.35	0.79	0.39
<sup>79</sup> Zn	1.61	0.61	-0.17	1.03	-0.02
<sup>80</sup> Ga	1.20	0.94	0.27	1.69	1.12
<sup>81</sup> Ga	2.08	1.22	0.74	1.65	1.18
<sup>94</sup> Rb	2.24	2.28	1.06	2.94	2.85
<sup>95</sup> Rb	2.69	3.23	1.89	3.85	3.33
<sup>129</sup> In	1.92	1.99	1.47	1.70	1.97
<sup>130</sup> In	1.90	2.27	1.87	2.03	2.30

a) Ref. 11)

b) Ref. 12)

c) Ref. 13)

d) Ref. 14)

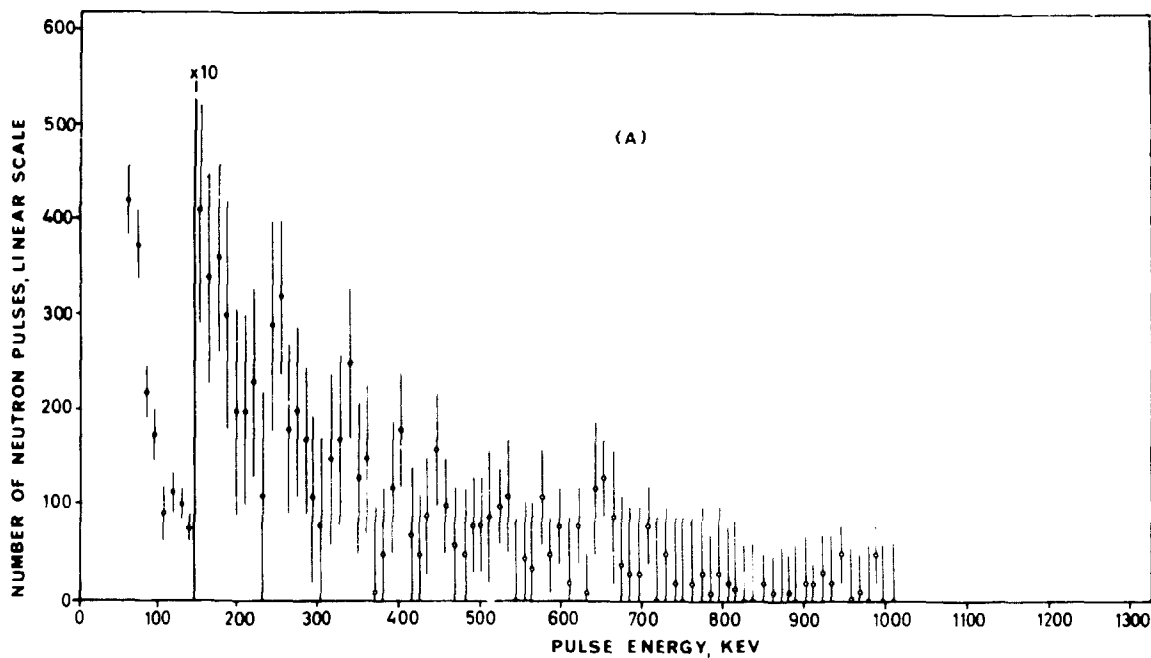
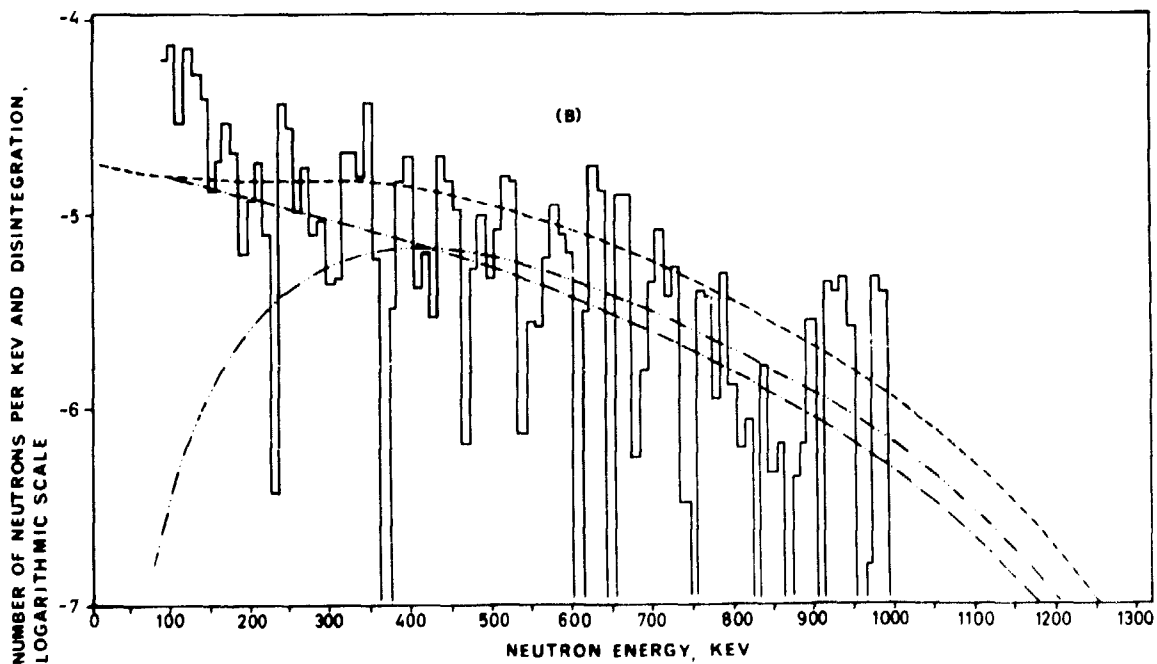


Fig. 1 (A) Experimental pulse spectrum for the precursor  $^{79}\text{(Zn,Ga)}$ .  
 Error bars in this and the following figures correspond to  $\pm$  one standard deviation.



(B) Histogram: Deduced neutron energy distribution assuming the  $P_n$ -value to be 1% (it is unmeasured).  
 Dashed curve: Calculated spectrum (for  $^{79}\text{Ga}$ ).  
 Dash-dot curve: p-wave component (for  $^{79}\text{Ga}$ ).  
 Dash-dot-dot curve: f-wave component (for  $^{79}\text{Ga}$ ).

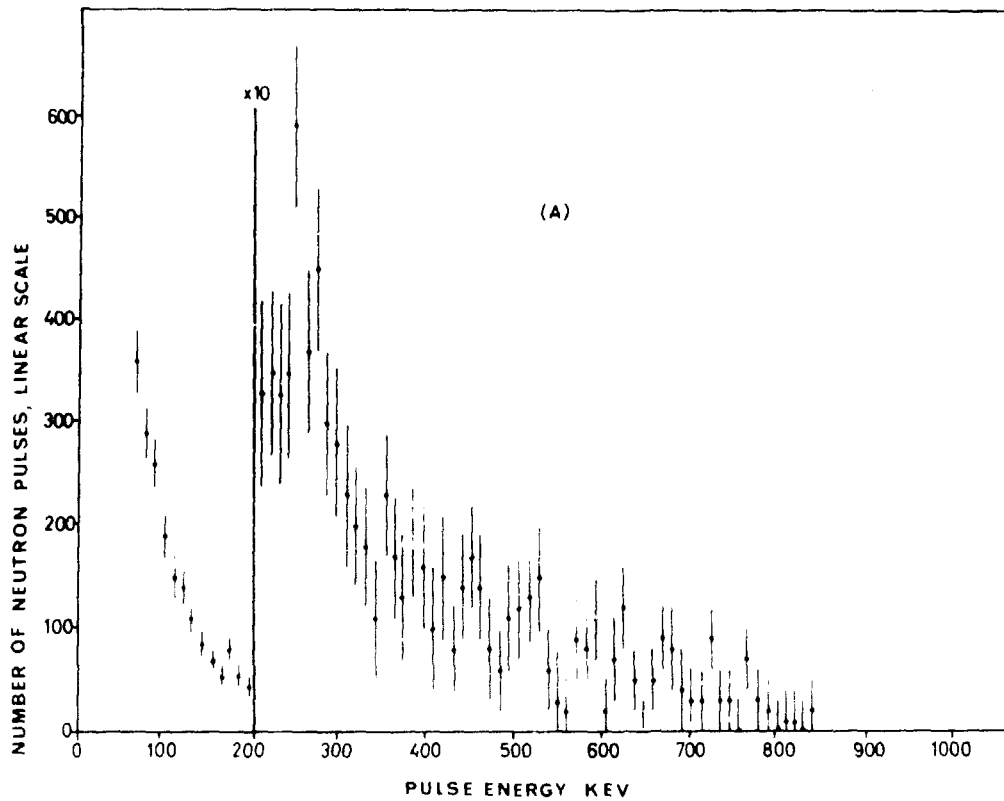
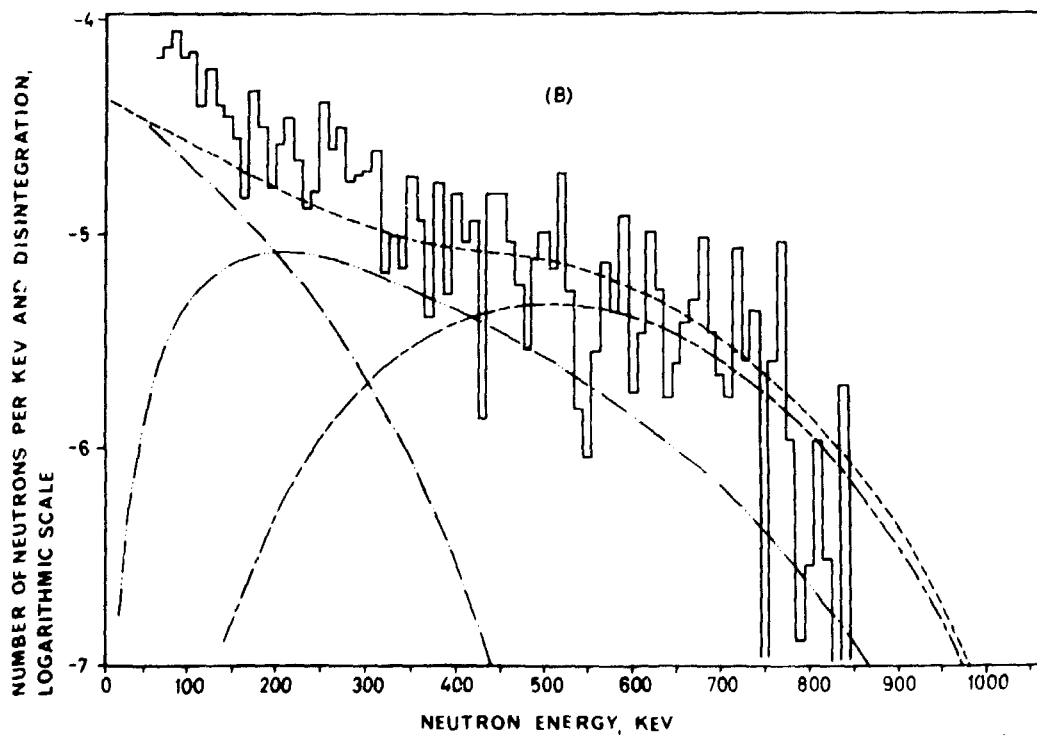


Fig. 2 (A) Experimental pulse spectrum for the precursor  $^{80}\text{Ga}$ .



(B) Histogram: Deduced neutron energy distribution assuming the  $P_n$ -value to be 10% (it is unmeasured).  
Dashed curve: Calculated spectrum.

Dash-dot curve: s-wave component feeding a hypothetical excited level at 500 keV.  
Dash-dot-dot curve: d-wave component.  
Large dash-small dash curve: g-wave component.

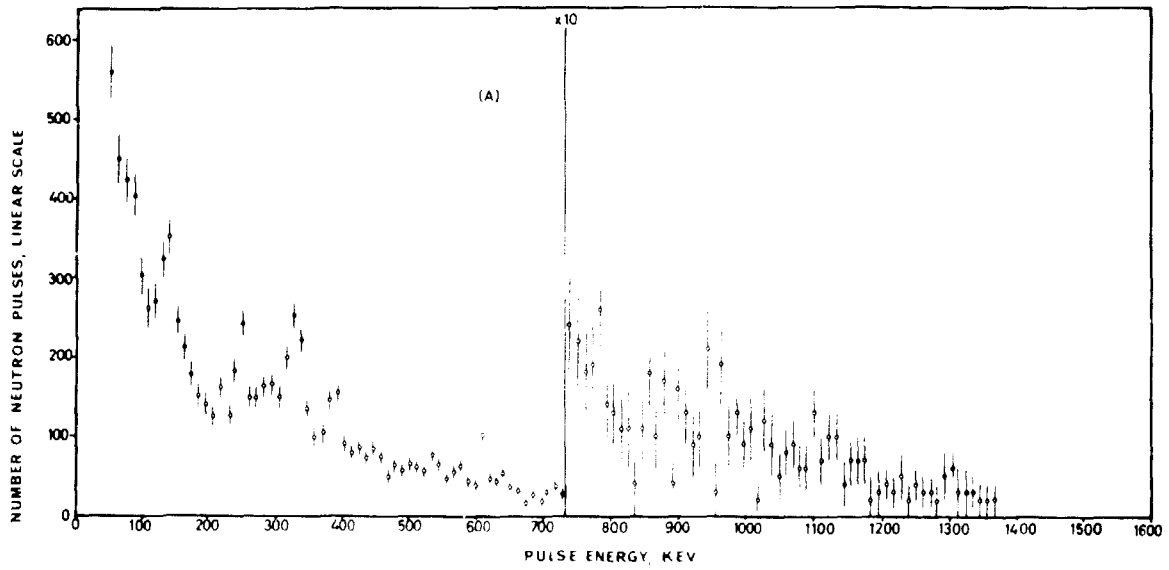
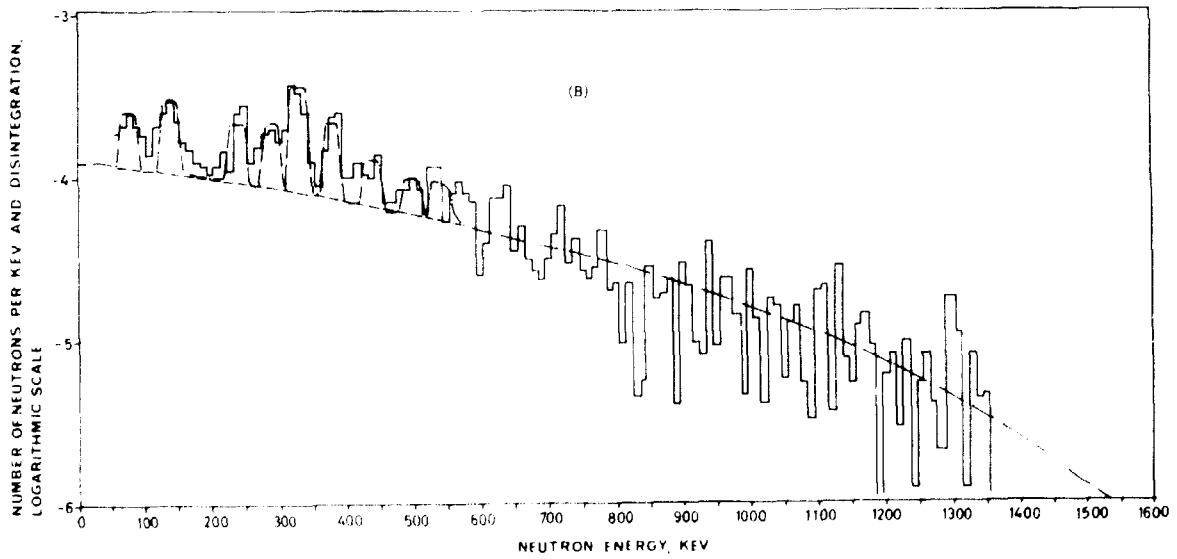


Fig. 3 (A) Experimental pulse spectrum for  $^{81}\text{Ga}$ .



(B) Histogram: Deduced neutron spectrum assuming the  $P_n$ -value to be  $10^{-7}$  (it is unmeasured).  
 Dash-dot curve: Calculated spectrum.  
 Dashed curve: p-wave component.



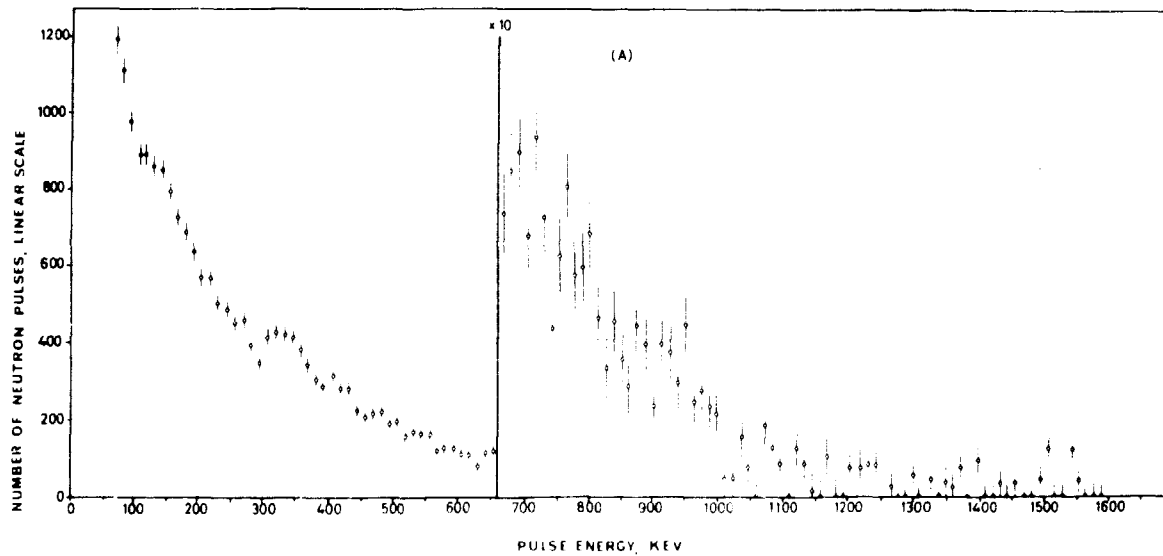
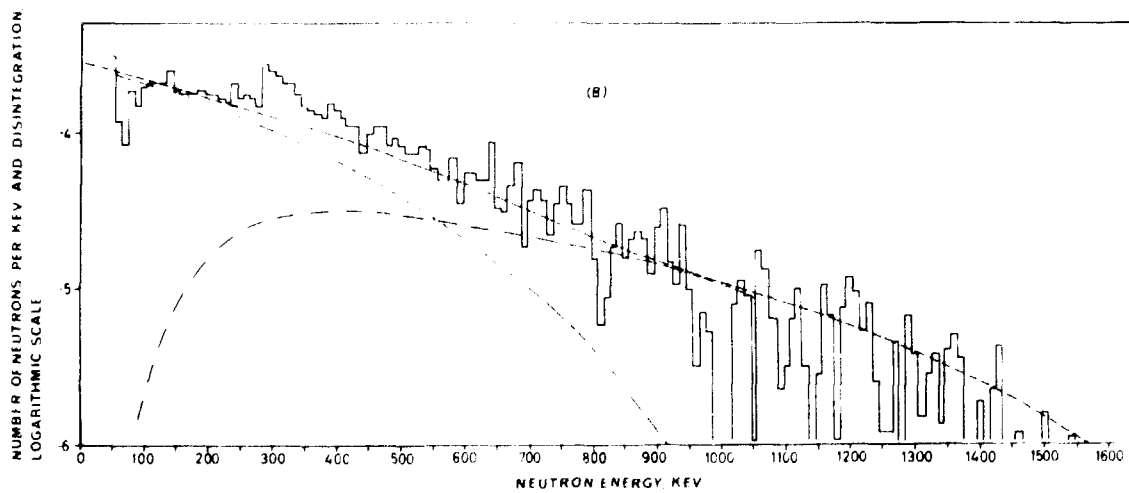


Fig. 4 (A) Experimental pulse spectrum for  $^{94}\text{Rb}$ .



(B) Deduced neutron spectrum using the experimental  $B_n$ -value of  $9.6 Z^{24}$ .

Dashed curve: Calculated spectrum.

Dash-dot curve: p-wave component feeding a hypothetical excited level at 1 MeV.

Dash-dot-dot curve: f-wave component.

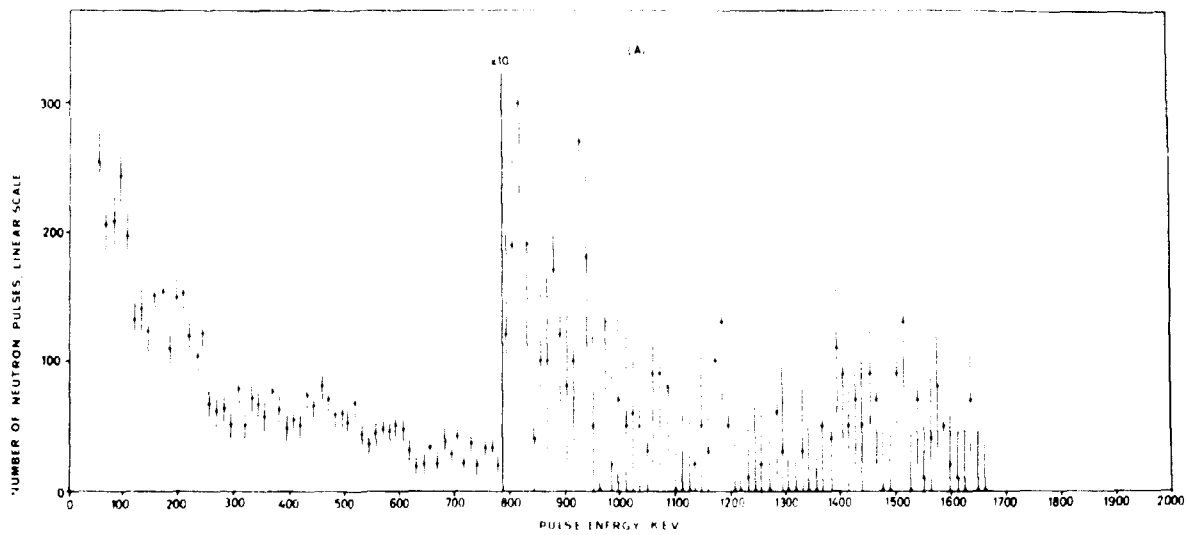
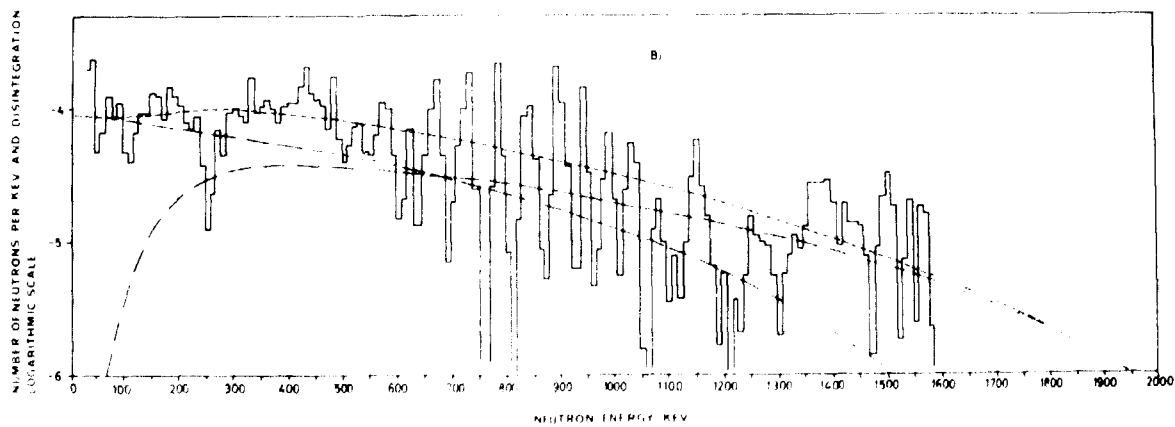


Fig. 5 (A) Experimental pulse spectrum for  $^{95}\text{Rb}$ .



(f) Histogram: Deduced neutron spectrum using the experimental  $B_n$ -value of  $8.4 \pm 24$ .

Dashed curve: Calculated spectrum

Dash-dot curve: p-wave component feeding a hypothetical excited level at 600 keV.

Dash-dot-dot curve: i-wave component.

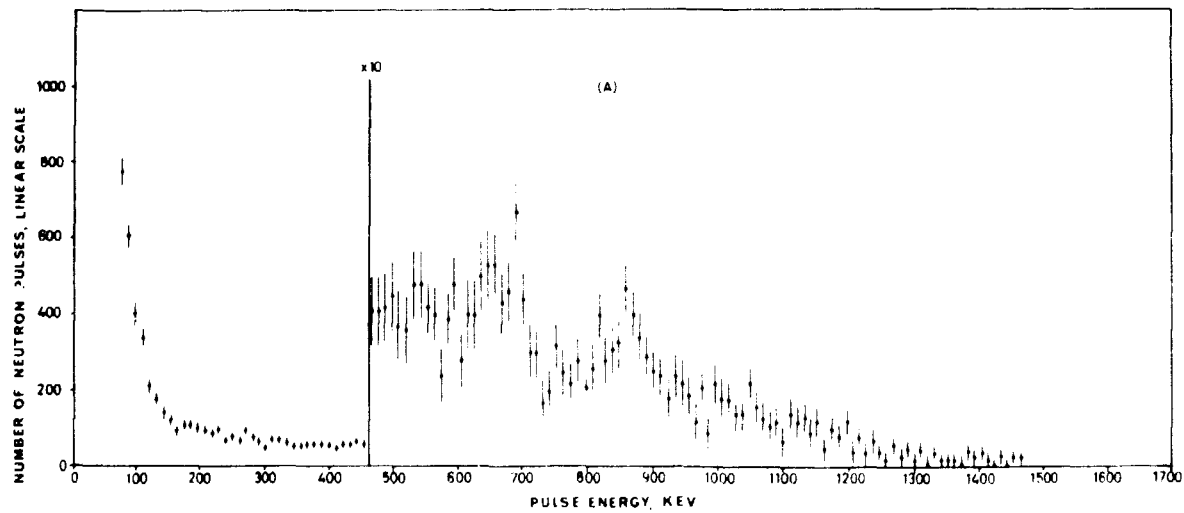
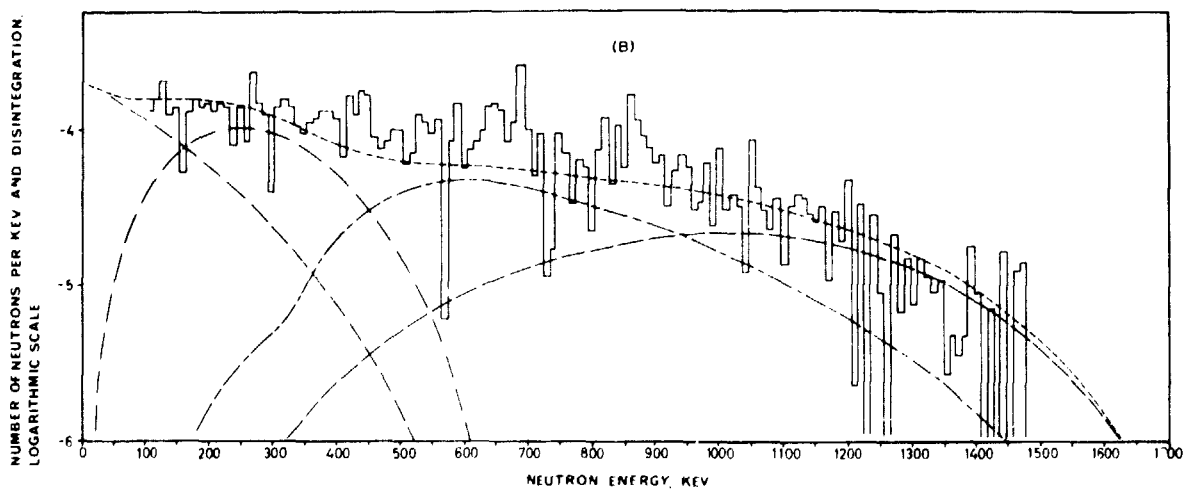


Fig. 6 (A) Experimental pulse spectrum for  $^{129}\text{In}$ .



(B) Deduced neutron spectrum assuming the  $\beta_n$ -value to be 10% (it is unmeasured).

Dashed curve: Calculated spectrum.

Dash-dot curve: p-wave component feeding an excited level at 1169 keV.

Dash-dot-dot curve: d-wave component feeding an excited level at 1169 keV.

Large dash-small dash curve: f-wave component.

Large dash curve: g-wave component.

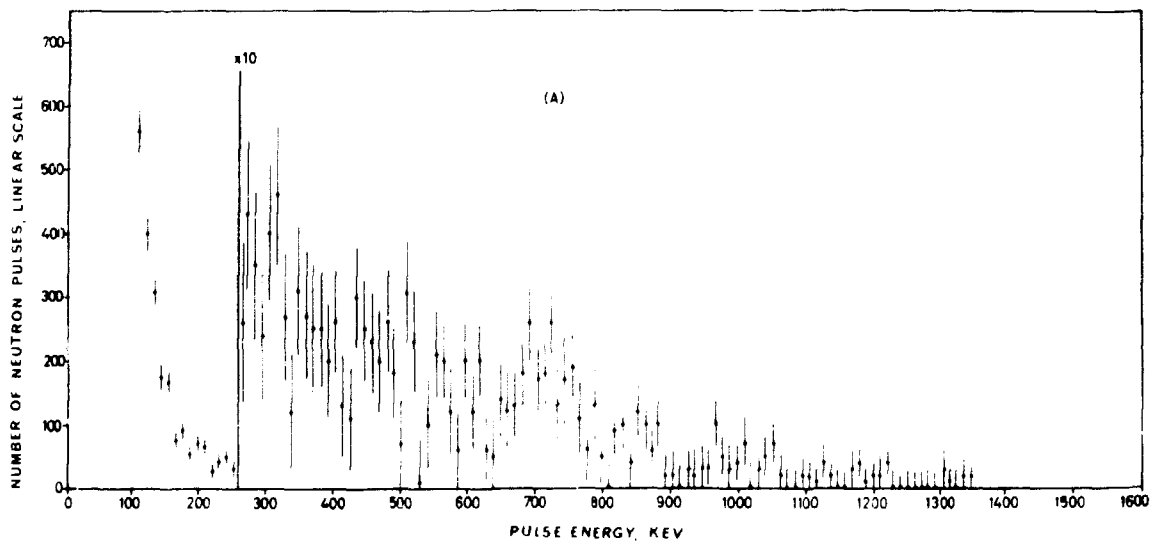
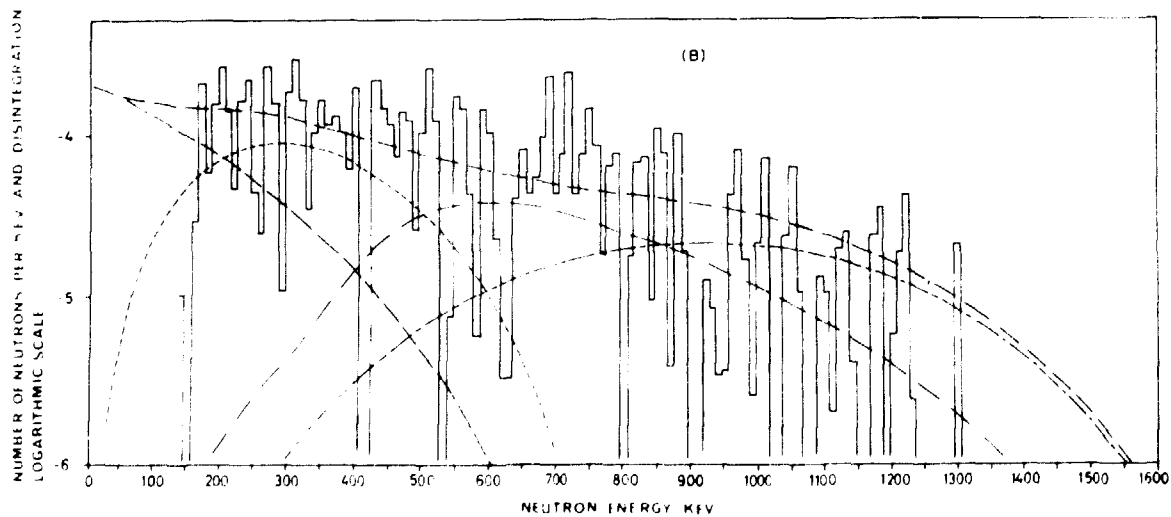


Fig. 7 (A) Experimental pulse spectrum for  $^{130}\text{In}$ .



(B) Histogram: Deduced neutron spectrum assuming the  $P_n$  value to be 10% (it is unmeasured).  
 Dash-dot curve: Calculated spectrum.  
 Large dash curve: s-wave component feeding an excited level at 1044 keV.  
 Small dash curve: d-wave component feeding an excited level at 1044 keV.  
 Dash-dot-dot curve: f-wave component.  
 Large dash-small dash curve: g-wave component.